ResearchGate

See discussions, stats, and author profiles for this publication at: https://www.researchgate.net/publication/224322512

Measurement of Magnetic Field Distorting the Electron Beam Direction in Scanning Electron Microscope

Article *in* IEEE Transactions on Instrumentation and Measurement · February 2009

DOI: 10.1109/TIM.2008.928415 · Source: IEEE Xplore

CITATIONS
3

READS
323

4 authors:

Mariusz Pluska
Institute of Electron Technology

65 PUBLICATIONS **181** CITATIONS

SEE PROFILE

Lukasz Oskwarek
Warsaw University of Technology

12 PUBLICATIONS **21** CITATIONS

SEE PROFILE

Remigiusz Rak
Warsaw University of Technology

128 PUBLICATIONS **316** CITATIONS

SEE PROFILE

Andrzej Czerwinski
Institute of Electron Technology

120 PUBLICATIONS **493** CITATIONS

SEE PROFILE

Some of the authors of this publication are also working on these related projects:

Automatic Detection of SSVEP using Independent Component Analysis View project

Recent lead-free solder alloys- testing and reliability View project

All content following this page was uploaded by Andrzej Czerwinski on 20 August 2014.

The user has requested enhancement of the downloaded file.

Measurement of Magnetic Field Distorting the Electron Beam Direction in Scanning Electron Microscope

Mariusz Pluska, Łukasz Oskwarek, Remigiusz J. Rak, and Andrzej Czerwinski

***Abstract*—The magnetic field that is generated by different electric devices in an environment of a scanning electron microscope (SEM) causes the direction of the electron beam to become distorted and, consequently, registered images to become distorted. This paper describes a method for a measurement of the magnetic field affecting the direction of the electron beam. It consists of the analysis of SEM images that are registered for several distances between the final aperture of an electron column and a specimen. Means of the measurement of a constant and a periodic magnetic field are explained. The presented examples show the results of the measurement of the constant field that is generated by coils that are placed either inside or outside the microscope chassis. The results are compared with the ones obtained using a reference magnetometer. In the presented method, a direct magnetic field influence on the electron beam is separated from any other influences. Also, the magnetic field nonuniformity along the electron beam path is considered. The current investigations enable the magnetic field compensation and test the shielding efficiency of the SEM chassis.**

***Index Terms*—Distortion, electromagnetic interference (EMI), electron beam deflection, electron microscopy, magnetic field measurement, magnetic fields.**

I. Introduction

MEASUREMENTS in electron microscopy are exposed to distortions of different kinds. The most frequent reason for image deformations in scanning electron microscopy (SEM) is electromagnetic interference (EMI) [1]. There are two main types of solutions for the elimination of SEM distortions—hardware- and software-based solutions. In the hardware-based solutions, the distortions are compensated with systems for magnetic field cancellation and/or reduced with multilayer electric/magnetic shields [2]–[4]. The software-based approach utilizes digital image processing to correct the deformed SEM images [5], [6].

Although the place for a microscope installation is usually selected carefully, and it obeys the manufacturer conditions, in practice, adding new equipment near the microscope system can make the environmental conditions much worse. Moreover, these conditions change depending on the power and the capacitive or inductive character of the load of devices that are actually working. For example, much stronger distortions are generated by devices with the inductive load than by devices with the resistive or capacitive load. Also, the distribution of the magnetic field of distortions changes. In the currently available systems for magnetic field cancellation, only the mean value of the field is measured. This is probably the reason for their poor stability. The hardware-based solutions are usually very complex and expensive. The increase in their stability and the main reduction in their cost can be gained when the distortions are eliminated or compensated selectively in the elements of the SEM system that are most sensitive to interference. Together with the additional application of the digital image correction, building a microscope system that is resistant to distortions is enabled.

The aim of the current investigation is to determine the density of the magnetic field flux that deflects the electron beam in the SEM and causes image distortions. For this purpose, a method that allows the measurement of the magnetic field with the use of the SEM itself is proposed. The method utilizes an electron beam as a magnetic field sensor without using any additional devices serving as meters. The advantage of this method is the consideration of the nonuniformity of the magnetic field interaction with the electron beam.

Techniques for the direct measurement of the magnetic field that utilizes coils, flux gates, Hall sensors, etc., cover a wide range of detectable field density and frequency [7]. Unfortunately, their application for the described purpose requires placing the sensor probe inside the SEM, near the electron beam, which is usually complicated, expensive, or, sometimes, even impossible. A technique for the measurement of the magnetic field in the SEM, based on the analysis of the deformation of the reference specimen image, was introduced [8], [9] and applied practically [10]. The technique enabled a measurement of an approximately uniform and constant magnetic field, which is generated by an investigated object that is placed near a reference specimen surface. It provided a valuable concept; however, its application for the measurement of the externally generated magnetic field required the consideration of the field nonuniformity. In the present approach, a number of SEM images for several lengths of the electron beam path are registered, which enables taking into account the nonuniform distribution of the magnetic field density along the electron beam path.

Manuscript received July 4, 2007; revised June 22, 2008. First published August 1, 2008; current version published December 9, 2008. The Associate Editor coordinating the review process for this paper was Dr. Richard Thorn.

M. Pluska is with the Institute of Theory of Electrical Engineering, Measurement and Information Systems, Warsaw University of Technology, 00-661 Warsaw, Poland, and also with the Institute of Electron Technology, 02-668 Warsaw, Poland (e-mail: mpluska@iem.pw.edu.pl; mpluska@ite.waw.pl).

Ł. Oskwarek and R. J. Rak are with the Institute of Theory of Electrical Engineering, Measurement and Information Systems, Warsaw University of Technology, 00-661 Warsaw, Poland (e-mail: rakrem@iem.pw.edu.pl).

A. Czerwinski is with the Institute of Electron Technology, 02-668 Warsaw, Poland (e-mail: aczerwin@ite.waw.pl).

Digital Object Identifier 10.1109/TIM.2008.928415

0018-9456/$25.00 © 2008 IEEE

Authorized licensed use limited to: POLITECHNIKI WARSZAWSKIEJ. Downloaded on December 10, 2008 at 02:33 from IEEE Xplore. Restrictions apply.

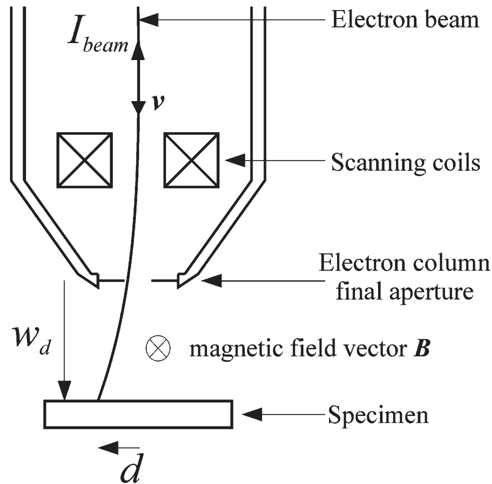

Fig. 1. Electron beam deflected along the working distance w_d by the magnetic field $\mathbf{B}$ that is perpendicularly directed to the plane of the page (crossing the page). By convention, the directions of the electron beam current I_{beam} and the electron velocity $\mathbf{v}$ are opposite.

In the general case, EMI influences several components of the SEM system [11]. The described method separates the distortions, which are caused by the direct influence of the magnetic field on the electron beam, from the other distortions (e.g., distortions of electric signals in the scanning block of the SEM). This enables the determination of the constant or periodic magnetic field that distorts the direction of the electron beam. Since the inertia of electrons is low, the proposed method is applied in the same way for constant and alternating fields.

II. Method

In an SEM, the electron beam is formed under a high vacuum in an electron column (also called the SEM column), and the investigated object is placed under a lower vacuum in a specimen chamber (also called the SEM chamber). A final aperture of the electron column reduces the pressure equalization. Electrons that are emitted from a cathode are accelerated in the electric field. The accelerating voltage in the SEM is typically in the range of 2–30 kV. A magnetic condenser lens that is placed in the middle of the SEM column, together with a number of apertures, controls the current of the electron beam I_{beam}. The external magnetic field penetrating the column may cause the center of the electron beam to miss the center of one of the apertures. In this case, some electrons do not pass through the aperture, which results in a decrease in the electron beam current and, consequently, a decrease in the brightness of SEM images. However, the current investigations showed that only the very strong field (hundreds of milliteslas) can cause such an effect, which means that, in practical conditions (in the range of 1 μT), it is negligible.

In the SEM column, the electron beam is focused by the magnetic final lens. Scanning coils, which are placed at the bottom of the electron column, sweep the beam over a specimen surface. Fig. 1 shows a very simplified diagram of the electron beam path between the scanning coils and the specimen. The direction of electron beam current I_{beam} is, by convention, the opposite of electron velocity $\mathbf{v}$. The magnetic field that penetrates the SEM column and the chamber deflects the electron beam due to Lorentz force law. At each point of the beam, Lorentz force vector $\boldsymbol{F}$ is perpendicular to magnetic field vector $\boldsymbol{B}$ and electron velocity vector $\mathbf{v}$ [12]. The distortions negligibly affect the magnitude of the $\mathbf{v}$ vector because it mainly results from the electron kinetic energy. In the SEM, it is typically in the range of 2–30 keV, which corresponds to the electron velocity in the range of 8%–30% of the speed of light. The magnitudes of the $\boldsymbol{F}$ and $\boldsymbol{B}$ vectors are proportional. When the magnetic field of distortions is generated externally, the shielding efficiency of various parts of the microscope chassis is different; therefore, the influence of the field on particular sections of the electron beam path is also different. Final beam deflection d is an integration of particular deflections along the electron beam path.

Generally, magnetic field vector $\boldsymbol{B}$ may go any direction in the 3-D space; however, only its two components that are perpendicular to the electron beam need to be measured. Due to Lorentz force law, the component of the magnetic field that is parallel to the electron movement does not affect the electron beam direction and, consequently, does not generate distortions. Above the final aperture, the magnetic field of distortions is superimposed on the field that is produced by the scanning coils. The only reason why Lorentz forces affect electrons that are below this aperture (i.e., within the SEM chamber) is the magnetic field of distortions.

The distance between the final aperture and the specimen surface, which is called working distance w_d, is usually changeable and measurable in the SEM. There are two pairs of scanning coils in the real microscope, and the electron beam is deflected twice in two opposite directions, which causes the beam deflection at the final aperture $(w_d = 0)$ to be typically equal to zero in cases without any distortions. However, practically, for the explanation of the current approach, the above simple model is adequate. In each moment, the scanning coils set the electron beam position at the specimen; however, this position is changed when the additional magnetic field is present. When the magnetic field magnitude changes slowly, the additional electron beam displacement is observable on SEM images as a movement of investigated objects. For periodic magnetic fields, a deformation of the object shapes appears.

Although the $\boldsymbol{B}$ vector has a nonuniform distribution along the electron beam path, in some narrow range of the working distance, it can be assumed as uniform. In this range, two orthogonal components, i.e., d_x and d_y, of additional beam deflection d caused by the Lorentz force $\boldsymbol{F}$ (F_x, F_y) can be expressed as follows:

$$d_x(w_d) = \frac{F_x}{2m_e v_e^2} w_d^2 + \frac{v_{x0}}{v_e} w_d + d_{x0} \tag{1a}$$

$$d_y(w_d) = \frac{F_y}{2m_e v_e^2} w_d^2 + \frac{v_{y0}}{v_e} w_d + d_{y0} \tag{1b}$$

where m_e is the electron mass, v_e is the velocity of the electron along the beam axis, v_{x0} and v_{y0} are two orthogonal components of the initial electron velocity caused by the force,

Authorized licensed use limited to: POLITECHNIKI WARSZAWSKIEJ. Downloaded on December 10, 2008 at 02:33 from IEEE Xplore. Restrictions apply.

and d_{x0} and d_{y0} are two orthogonal components of the initial beam displacement caused by the force. As we can notice, only the expression that stands by w_d^2 is directly connected with the Lorentz force and, as a result, with the magnetic field. To find the force that acts on the beam, components d_x and d_y of displacement d are measured for several working distances w_d (at least three), and the obtained characteristics are approximated with the following second-order polynomials:

$$d_x = a_x w_d^2 + b_x w_d + c_x \tag{2a}$$

$$d_y = a_y w_d^2 + b_y w_d + c_y \tag{2b}$$

where a, b, and c are the function parameters that correspond to their physical equivalents from (1a) and (1b). Assuming that the measured field is uniform along the range of used working distances, the above parameters are constant, and their determination demands solving a set of at least three equations for both directions. When we assign the point of final aperture to $w_d = 0$, the c parameter is the initial beam displacement, and the b parameter is proportional to the initial electron velocity in the direction that is parallel to the Lorentz force. Parameters a_x and a_y are proportional to the Lorentz force and, consequently, to the magnetic field magnitude, i.e.,

$$a_x = \frac{F_x}{2m_e v_e^2} \tag{3a}$$

$$a_y = \frac{F_y}{2m_e v_e^2}. \tag{3b}$$

As a result, the approximation gives a valuable separation of the field influence above the final aperture point (represented by the parameters b and c) from the influence below this point (represented by the parameter a). It has to be noticed that the calculation of the magnetic field value as being directly proportional to the beam displacement d as it was described in [7]–[9]—without considering different reasons of this displacement as in (1a) and (1b)—is possible only when the measured field is uniform along the whole electron beam path. This is not the case, as even a uniform external field would be differently shielded by various parts of the microscope chassis. The x and y indexes represent two orthogonal axes of the plane that is perpendicular to the electron beam axis (with the plane being parallel to the specimen surface). Orientations of these orthogonal axes may be assumed arbitrarily. Complying with the fact that electron velocity v_e along the column axis is given by

$$v_e = \sqrt{2E/m_e} \tag{4}$$

time t of the electron movement along the working distance is given by

$$t = w_d/v_e \tag{5}$$

and the Lorentz force for a single electron is given by

$$\mathbf{F} = e\mathbf{v}_e \times \mathbf{B} \tag{6}$$

then two perpendicular components of the magnetic field vector can be calculated as follows:

$$B_y = \frac{a_x\sqrt{8Em_e}}{e} \tag{7a}$$

$$B_x = \frac{a_y\sqrt{8Em_e}}{e} \tag{7b}$$

where m_e is the relativistic electron mass (in kilograms), e is the electron charge (in coulombs), and E is the electron energy (in joules). It has to be noticed that beam deflection d_x along the x-axis, from which the a_x parameter is calculated, is generated by the B_y component of the magnetic field vector. The same situation occurs for the perpendicular direction. Since velocity v_e of the beam electrons is comparable with the speed of light in a vacuum c_v (for $E = 10$ keV and $v = 0.19c_v$), the relativistic mass gain should be taken into consideration, i.e.,

$$m_e = m_{e0}/\sqrt{1 - v_e^2/c_v^2} \tag{8}$$

where m_{e0} is the electron mass at $v_e = 0$. Finally, magnitude B of the magnetic field can be determined, i.e.,

$$B = \sqrt{B_x^2 + B_y^2}. \tag{9}$$

Decreasing the span of several used working distances gives a higher probability of reaching magnetic field uniformity at a specified range. However, when the magnetic field is nonuniform along the used range of working distances, its mean value is measured. Repeating the measurements for several narrow ranges of the working distance enables the measurement of the field changes between this range and considers its nonuniformity. The maximal range of working distances in most of the SEM is about a few centimeters. The above method allows measuring the reference, the constant magnetic field, or the periodic magnetic field.

In the case of the constant field, the beam displacement is measured by comparing two images of any characteristic element of the specimen that is being registered with and without the presence of the magnetic field. The difference between the position of the element on the images is equal to the electron beam displacement $d(w_d)$ (Fig. 2).

An alternating magnetic field periodically deflects the electron beam. The time of a single-line scan can be set many times shorter than the period of the distorting magnetic field. The image deformation is then almost constant for each separate scan line, and the edge deformation becomes recognizable after scanning many lines. Obviously, determining both perpendicular components of the magnetic field is necessary. A periodic deformation of vertical edges is caused by the Lorentz force that is directed along the horizontal scan lines (Fig. 3). It involves this component of the magnetic field vector that is perpendicular to the scan line. Therefore, the measurement of the alternating magnetic field needs to be performed for two perpendicular scanning directions. The specimen should contain at least one observable edge. The only limitation is that the shape of this edge should not be very wavy itself. Such a wavy shape could be misinterpreted as a result of magnetic distortions. An irregular shape of the edge is allowed, provided

Authorized licensed use limited to: POLITECHNIKI WARSZAWSKIEJ. Downloaded on December 10, 2008 at 02:33 from IEEE Xplore. Restrictions apply.

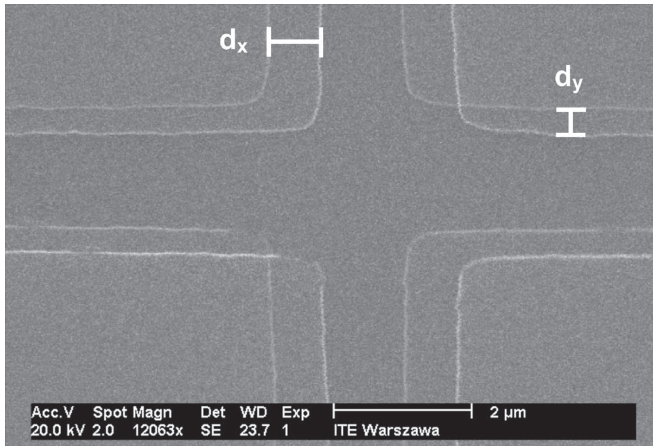

Fig. 2. Superposition of SEM images registered with and without the presence of the magnetic field. Working distance $w_d = 23$ mm. The perpendicular displacements d_x and d_y of the object on the image are marked.

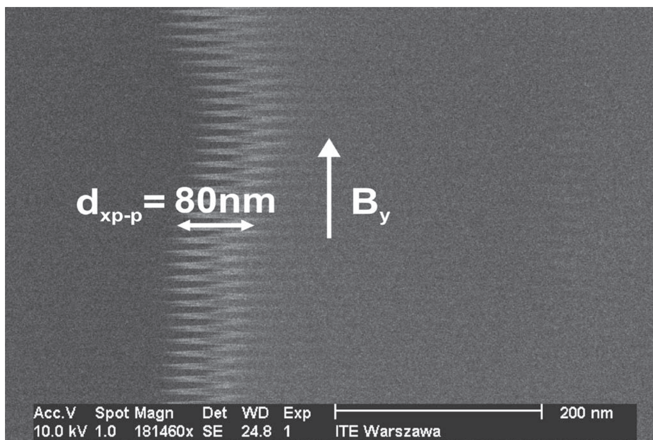

Fig. 3. Specimen edge deformation caused by a periodic ($f = 50$ Hz) magnetic field. Peak-to-peak deformation $d_{xp\text{-}p}$, with the edge blur considered, and the B_y component of magnetic field vector $\mathbf{B}$ are marked.

that the periodic deformation has to be distinguished from the edge irregularity itself. For a comparatively small irregularity, the amplitude of the deformations can be determined in a similar way as for a regular edge. Fig. 3 presents an example of deformations of such a slightly irregular edge. In cases when specimen edges are more irregular, the edge-detection algorithm and the Fourier transform of its result can be applied for the separation of the edge shape from the periodic image deformations and for the determination of their amplitude [6]. Most of the distortions in the SEM are generated by the magnetic field of power devices at a frequency of 50–60 Hz. To obtain a clearly visible periodic deformation of images, a frequency of the vertical scan generator should be at least a few times lower than the distortion frequency. As mentioned before, measurements of the alternating magnetic field are performed in two steps.

In the first step, the direction of scanning should be set to obtain the vertical orientation of the edge on the image (while the scan direction with regard to the image is usually horizontal). In this case, the component of the magnetic field that is perpendicular to the scan direction deforms the edge to the characteristic wavy pattern (Fig. 3). The peak-to-peak value

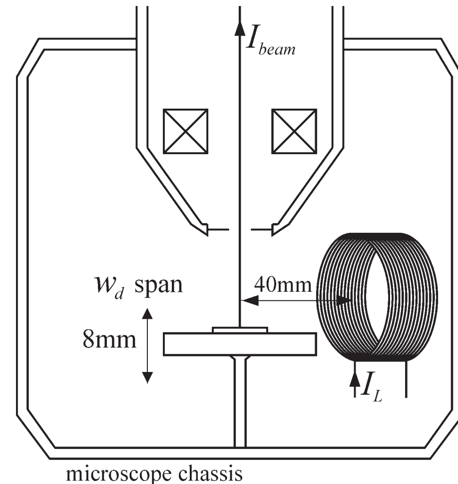

Fig. 4. Placement of the small inductor inside the SEM chamber.

of the edge deformation ($d_{xp\text{-}p}$) is equal to the peak-to-peak value of the electron beam displacement. The measurements can be performed on the condition that the periodic deformation is visible, i.e., when the image resolution enables an observation of the edge-shape changes. Larger deformations can be measured more precisely because a relative error caused by the inaccuracy due to the image discretization (equal to ± 1 pixel) is smaller.

In the second step, the right angle rotation of the specimen and the simultaneous change of the scanning direction also allow for the measurement of the peak-to-peak displacement value $d_{yp\text{-}p}$ for the perpendicular direction using the observed distortions of the same edge, which is now being rotated. This displacement corresponds to the perpendicular component of the magnetic field vector. The approximation with the second-order polynomial [see (2a)] of the first measured characteristic $d_{xp\text{-}p} = f(w_d)$ is used to determine the peak-to-peak magnetic field value $B_{yp\text{-}p}$. The same approach [using (2b)] is applied for the perpendicular direction.

An interesting observation is that it is usually possible to set the specimen orientation and the scanning direction in such a manner that the distortions appear on the image only for one direction. In this case, when both the specimen and the scanning direction are right-angle-rotated afterward, the observed edge has no distortions. The occurrence of such an effect confirms that there is only one dominant source of distortions, and that the distinguished direction is related to the magnetic field line of this source.

III. Application Examples

A measurement procedure for the constant magnetic field, the reference magnetic field, and the periodic distortions will be described. The investigations were performed using a Philips XL-30 scanning electron microscope. The reference field was generated either inside or outside the SEM chamber.

In the first case, a small coil with a diameter of 23 mm was placed inside the SEM chamber (Fig. 4). The coil was perpendicularly directed to the electron beam in such a way that its axis of symmetry crossed the electron beam. The distance

Authorized licensed use limited to: POLITECHNIKI WARSZAWSKIEJ. Downloaded on December 10, 2008 at 02:33 from IEEE Xplore. Restrictions apply.

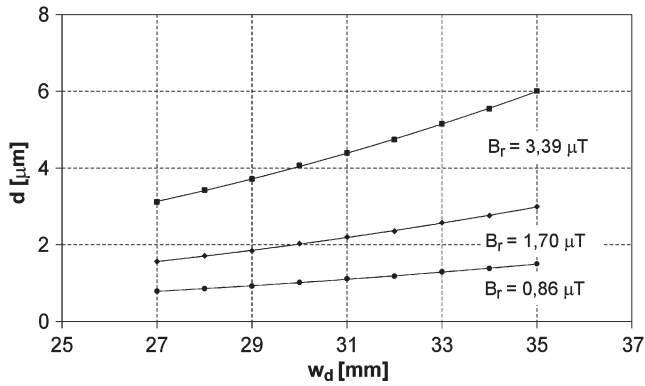

Fig. 5. Measurement results for the magnetic field of 0.86, 1.70, and 3.39 μT that are generated by the small coil inside the SEM chamber. Electron beam energy $E = 2$ keV.

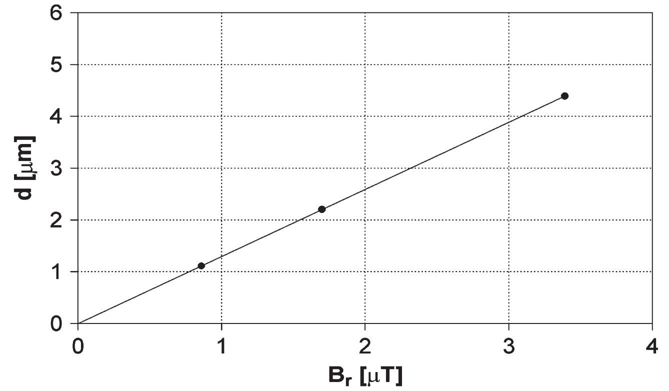

Fig. 7. Electron beam displacement d versus magnetic field B measured at a working distance of 31 mm.

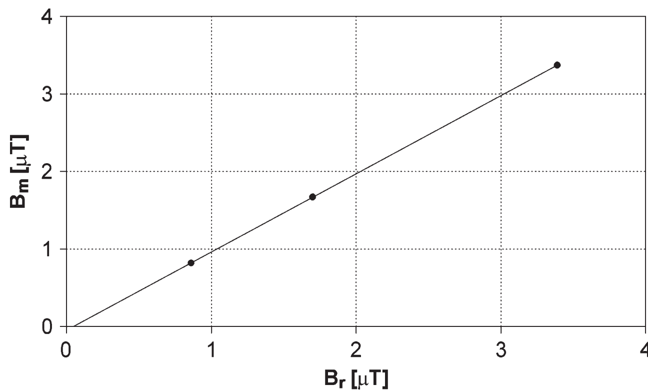

Fig. 6. Results B_m of magnetic field measurements with the current approach versus results B_r obtained from the reference magnetometer.

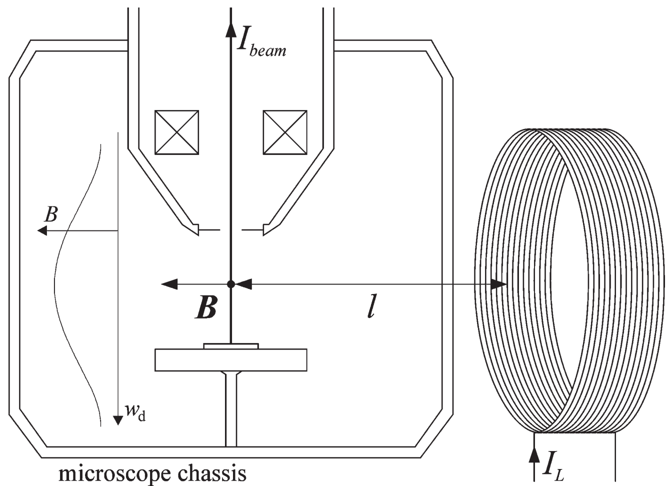

Fig. 8. Placement of the external coil toward the SEM chamber. The distance l between the coil face and the electron is marked. The magnitude nonuniformity of the $\mathbf{B}$ vector versus working distance w_d is shown.

between the coil face and the electron beam axis was about 40 mm. For electron energy $E = 2$ keV and three values of the coil current I_L (0.16, 0.33, and 0.66 mA), the electron beam displacement versus working distance was measured (Fig. 5). The x and y coordinates were assumed in such a way that the displacement $d_y = 0$, and the total displacement $d(w_d) = d_x(w_d)$. The a_x parameters of (1a) were estimated: $a_{x1} = 2.65 \times 10^{-3}$ (1/m), $a_{x2} = 5.40 \times 10^{-3}$ (1/m), and $a_{x3} = 10.91 \times 10^{-3}$ (1/m), which correspond to the magnetic field values $B_1 = 0.82$ μT, $B_2 = 1.67$ μT, and $B_3 = 3.37$ μT, respectively.

The magnetic field generated with the coil was also measured with an MT-100 magnetometer. The measurement consisted of replacing the specimen with the magnetic field sensor of MT-100 in the open SEM chamber. The results for the same coil currents were $B_1 = 0.86$ μT, $B_2 = 1.70$ μT, and $B_3 = 3.39$ μT. Fig. 6 shows the results obtained with the presented method (B_m) versus the results achieved from the magnetometer (B_r). Fig. 7 presents electron beam displacement d versus magnetic field B_r for working distance $w_d = 31$ mm. Both characteristics (Figs. 6 and 7) are linear.

The influence of the external constant magnetic field on the electron beam was also measured. In this case, a coil, with a diameter of 90 mm, was placed outside the SEM chamber (Fig. 8). The distance between the face of the coil and the electron beam was 25 cm. The I_L current was set to 0.7 mA. It has been measured, using MT-100, that the maximum flux density that was produced by the coil at the specified distance (along its axis of symmetry) was 4.9 μT. However, the chassis significantly reduced the field inside the SEM chamber. SEM images were registered for several different values of working distance w_d with and without the reference magnetic field. The electron beam displacements d_x and d_y were measured for two perpendicular directions. These measurements were repeated for different electron energies E to test the method repeatability and the conformity of the results.

An interesting observation can be drawn from the example measurement results shown in Fig. 9. The linear and squared components of deformations are generally related to the magnetic fields that are, respectively, present either in the SEM column (i.e., above the final aperture) or in the SEM chamber (i.e., below the final aperture). Therefore, in all cases, the measured characteristics consist of both linear and squared components, related to the e-beam paths, above and below the final aperture, respectively. The $dx = f(wd)$ dependence shown in Fig. 9, which is related to one component of the magnetic field, clearly has a squared character. The $dy = f(wd)$ characteristics, which are related to the field component that is

Authorized licensed use limited to: POLITECHNIKI WARSZAWSKIEJ. Downloaded on December 10, 2008 at 02:33 from IEEE Xplore. Restrictions apply.

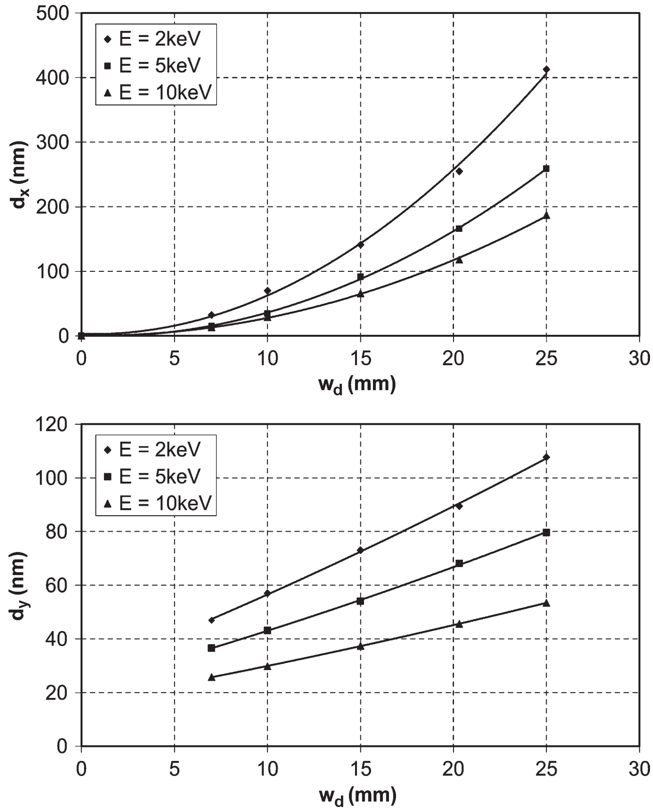

Fig. 9. Measured dependence of the magnetic-field-generated electron beam displacements (d_x, d_y) on working distance w_d at three different electron beam energies E: 2, 5, and 10 keV.

perpendicular to the first one, are also described by quadratic functions, but their linear parts are comparatively much stronger. The difference in the field impact between both perpendicular directions is probably caused by the shielding efficiency of the different parts of the microscope. The shielding efficiency of the cylindrical chassis of the microscope column, which is applied above the final aperture, is uniform, whereas the shielding efficiency of the cubic chamber chassis, which is applied below the final aperture, depends on the magnetic field direction. Regardless of the different shielding efficiencies, the measurement results are not affected by the observed linearity of the characteristics because only the quadratic parts of the deformations are considered in the measurements of the magnetic field that is present in the SEM chamber. From these results, the a_x and a_y parameters for two perpendicular directions and the corresponding components of the magnetic field vector were calculated as follows:

$$a_{x,2\,\mathrm{keV}} = 7.12 \times 10^{-4}\ (1/\mathrm{m}) \rightarrow B_{y,2\,\mathrm{keV}} = 219.78\ \mathrm{nT}$$

$$a_{x,5\,\mathrm{keV}} = 4.45 \times 10^{-4}\ (1/\mathrm{m}) \rightarrow B_{y,5\,\mathrm{keV}} = 219.87\ \mathrm{nT}$$

$$a_{x,10\,\mathrm{keV}} = 3.10 \times 10^{-4}\ (1/\mathrm{m}) \rightarrow B_{y,10\,\mathrm{keV}} = 220.84\ \mathrm{nT}$$

$$a_{y,2\,\mathrm{keV}} = 1.9 \times 10^{-5}\ (1/\mathrm{m}) \rightarrow B_{x,2\,\mathrm{keV}} = 7.1\ \mathrm{nT}$$

$$a_{y,5\,\mathrm{keV}} = 1.6 \times 10^{-5}\ (1/\mathrm{m}) \rightarrow B_{x,5\,\mathrm{keV}} = 7.9\ \mathrm{nT}$$

$$a_{y,10\,\mathrm{keV}} = 1.0 \times 10^{-5}\ (1/\mathrm{m}) \rightarrow B_{x,10\,\mathrm{keV}} = 7.1\ \mathrm{nT}.$$

The magnitudes of the measured magnetic field vector were given as follows:

$$B_{2\,\mathrm{keV}} = 219.89\ \mathrm{nT}$$

$$B_{5\,\mathrm{keV}} = 220.01\ \mathrm{nT}$$

$$B_{10\,\mathrm{keV}} = 220.95\ \mathrm{nT}.$$

As can be seen, the field value that is calculated for different conditions had, in this case, very good conformity of results—the maximum difference between results is smaller than 0.5%. On the contrary, an estimation of the magnetic field directly from the electron beam displacement, with the method described in [7]–[9], leads to very poor conformity of the field magnitude that is calculated for different energies, as its value differs up to 34%.

Since the source magnetic field was equal to 4.9 μT and the measured value inside the microscope chamber was equal to 220 nT, the microscope chassis reduced the field by about 27 dB (22 times). The shielding is not uniform and depends on the field direction and the frequency. In the other measurements, the coil placement toward the SEM chassis was changed. The current of the coil was either constant or alternating with a frequency of 50 Hz. The shielding efficiency was in the range of 15–27 dB.

IV. Conclusion

The method that has been presented constitutes an important element in the process of the construction of the distortion-resistant microscope system. It allows for an easy and repeatable measurement of the magnetic field deflecting the electron beam inside an SEM chamber based on the analysis of registered images. Additionally, it enables the separation of other influences of the magnetic field besides this direct impact. The current purpose of the method is to determine how the external magnetic field acts on the electron beam; therefore, the detailed analysis of measurement accuracy is not crucial. However, the method has been verified by comparing its results (for the constant field) with the results obtained from the MT-100 magnetometer; the conformity of the results was satisfactory.

The magnetic field shielding by the microscope chassis is not uniform and depends on the field direction and the frequency. The revealed shielding efficiency was from 15 to 27 dB for different directions and frequencies of the magnetic field.

It has been observed that the parameters of the approximation polynomial [see (2a) and (2b)] that correspond to the physical parameters of the electron beam displacement depend on the localization of the magnetic field source. The aim of further work will be the identification of the distortion source by the analysis of the shape of the distortion signal and the revealed parameters of the approximation polynomial.

References

[1] A. E. Vladar, *Scanning electron microscopy in real world environment*, 2003. [Online]. Available: www.nanobuildings.com

[2] T. C. Isabell, *Analytical instrumentation facility requirements for nanotechnology*, 2004. [Online]. Available: www.nanobuildings.com

Authorized licensed use limited to: POLITECHNIKI WARSZAWSKIEJ. Downloaded on December 10, 2008 at 02:33 from IEEE Xplore. Restrictions apply.

[3] M. L. Hiles, R. G. Olsen, K. C. Holte, D. R. Jensen, and K. L. Griffing, "Power frequency magnetic field management using a combination of active and passive shielding technology," *IEEE Trans. Power Del.*, vol. 13, no. 1, pp. 171–179, Jan. 1998.
[4] K. C. E. Peng, Y. E. Pradeep, and C. T. Phock, "Image compensation device for a scanning electron microscope," U.S. Patent 6 791 083, Sep. 14, 2004.
[5] K. Homma, F. Komura, and T. Furuya, "An image correction method for vibrated scan of SEM (scanning electron microscope)," in *Proc. Int. Workshop Ind. Appl. Mach. Vis. Mach. Intell.*, 1987, pp. 26–30.
[6] M. Płuska, A. Czerwinski, J. Ratajczak, J. Kątcki, and R. Rak, "Elimination of scanning electron microscopy image periodic distortions with digital signal-processing methods," *J. Microsc.*, vol. 224, no. 1, pp. 89–92, Oct. 2006.
[7] P. Ripka, Ed., *Magnetic Sensors and Magnetometers*. Boston, MA: Artech House, 2001.
[8] R. M. F. Thornley and J. D. Hutchinson, "Magnetic field measurement in the scanning electron microscope," *Appl. Phys. Lett.*, vol. 13, no. 8, pp. 249–250, Oct. 1968.
[9] R. M. F. Thornley and J. D. Hutchinson, "Magnetic field measurements in the scanning electron microscope," *IEEE Trans. Magn.*, vol. MAG-5, no. 3, pp. 271–275, Sep. 1969.
[10] T. Ishiba and H. Suzuki, "Measurement of magnetic field of magnetic recording head by a scanning electron microscope," *Jpn. J. Appl. Phys.*, vol. 13, no. 3, pp. 457–462, 1974.
[11] M. Płuska, A. Czerwiñski, Ł. Oskwarek, and R. Rak, "Quantitative measurement of electromagnetic distortions in scanning electron microscope (SEM)," in *Proc. IEEE Inst. Meas. Technol. Conf.*, 2007, pp. 1–4.
[12] B. I. Bleaney and B. Bleaney, *Electricity and Magnetism*, 2nd ed. Oxford, U.K.: Clarendon, 1965.

Mariusz Pluska received the M.Sc. degree in 2003 from Warsaw University of Technology, Warsaw, Poland, where he is currently working toward the Ph.D. degree.

He is currently with the Department of Materials and Semiconductor Structures Research, Institute of Electron Technology, Warsaw. His research interests include digital signal processing, the reduction of distortions in scanning electron microscopy, and the development of advanced electron-microscopy-based methods for the characterization of semiconductor materials and devices.

Łukasz Oskwarek was born in Bielsko-Biała, Poland, in 1973. He received the B.S. degree from the Silesian University of Technology, Gliwice, Poland, in 1998 and the Ph.D. degree in electrical engineering from Warsaw University of Technology, Warsaw, Poland, in 2003.

Since December 2003, he has been with the Division of Measurement and Information, Warsaw University of Technology, as a Tutor. He has authored about 20 articles published in Polish and international scientific letters and conference materials. His research interests include multipoint and multisensor measurement systems, measurement accuracy estimation, digital signal processing, computer–human interaction, and biometry.

Remigiusz J. Rak received the M.Sc., Ph.D., and D.Sc. degrees from Warsaw University of Technology, Warsaw, Poland, in 1974, 1982, and 1998, respectively.

In 2004, he obtained the title of Professor. He is currently the Head of the Department of Information and Measurement Systems, Faculty of Electrical Engineering, Warsaw University of Technology. He is also a Rector's Delegate with the New Forms and Innovations of Education. His current research interests include time-frequency analysis, signal compression, networked-distributed measurement systems (virtual instruments and Internet-based virtual laboratories), and distance-learning models.

Andrzej Czerwinski received the M.Sc. degree from Warsaw University of Technology, Warsaw, Poland, in 1976 and the Ph.D. and D.Sc. degrees from the Institute of Electron Technology, Warsaw, in 1983 and 2002, respectively.

He is currently an Associate Professor and the Head of the Department of Materials and Semiconductor Structures Research, Institute of Electron Technology. His current research interests are mainly related to structural and electrical measurements and investigation methods for the evaluation of semiconductor materials and devices and the semiconductor microtechnology and nanotechnology.

Authorized licensed use limited to: POLITECHNIKI WARSZAWSKIEJ. Downloaded on December 10, 2008 at 02:33 from IEEE Xplore. Restrictions apply.